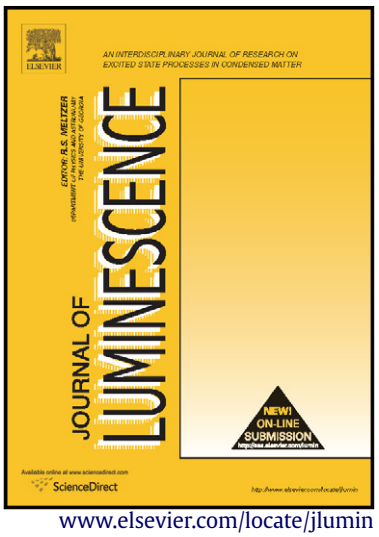

www.elsevier.com/locate/jlumin

Thermally stimulated luminescence of undoped and Ce^{3+}-doped Gd_2SiO_5 and $(Lu,Gd)_2SiO_5$ single crystals

V. Bondar, L. Grigorjeva, T. Kärner, O. Sidletskiy, K. Smits, S. Zazubovich, A. Zolotarjovs

PII: S0022-2313(14)00684-X
DOI: http://dx.doi.org/10.1016/j.jlumin.2014.11.034
Reference: LUMIN13034

To appear in: *Journal of Luminescence*

Received date: 8 May 2014
Revised date: 31 October 2014
Accepted date: 18 November 2014

Cite this article as: V. Bondar, L. Grigorjeva, T. Kärner, O. Sidletskiy, K. Smits, S. Zazubovich, A. Zolotarjovs, Thermally stimulated luminescence of undoped and Ce^{3+}-doped Gd_2SiO_5 and $(Lu,Gd)_2SiO_5$ single crystals, *Journal of Luminescence,* http://dx.doi.org/10.1016/j.jlumin.2014.11.034

Thermally stimulated luminescence of undoped and Ce^{3+}-doped Gd_2SiO_5 and $(Lu,Gd)_2SiO_5$ single crystals

V. Bondar [a], L. Grigorjeva [b], T. Kärner [c], O. Sidletskiy [a], K. Smits [b], S. Zazubovich [c*], A. Zolotarjovs [b]

[a] *Institute for Scintillation Materials, NAS of Ukraine, 60 Lenin Ave. 61001 Kharkiv, Ukraine*
[b] *Institute of Solid State Physics, University of Latvia, 8 Kengaraga St., Riga, LV-1063, Latvia*
[c] *Institute of Physics, University of Tartu, Ravila 14c, 50411 Tartu, Estonia*

ABSTRACT

Thermally stimulated luminescence (TSL) characteristics (TSL glow curves and TSL spectra) are investigated in the 4-520 K temperature range for the X-ray irradiated at 4 K, 8 K, or 80 K single crystals of gadolinium and lutetium-gadolinium oxyorthosilicates. The nominally undoped Gd_2SiO_5 and $(Lu,Gd)_2SiO_5$ crystals, containing traces of Ce^{3+}, Tb^{3+}, and Eu^{3+} ions, and Ce^{3+}-doped Gd_2SiO_5 and $(Lu,Gd)_2SiO_5$ crystals are studied. For the first time, the TSL glow curves of these materials are measured separately for the electron (intrinsic, Ce^{3+}- or Tb^{3+}-related) and hole (Eu^{3+}-related) recombination luminescence, and the TSL glow curve peaks, arising from thermal decay of various electron and hole centers, are identified. The origin of the traps related to the TSL peaks is discussed, and thermal stability parameters of the electron and hole traps are calculated.

Keywords: Thermally stimulated luminescence, electron and hole traps, single crystals of Gd_2SiO_5 and $(Lu,Gd)_2SiO_5$

* Corresponding author: *E-mail address*: svet@fi.tartu.ee (S. Zazubovich)

1. Introduction

Since the first publication [1], the Gd_2SiO_5:Ce (GSO:Ce) single crystal has been extensively studied as a promising scintillation material for applications in high energy physics, nuclear physics, tomographic medical X-ray imaging, gamma-ray detectors for positron emission tomography and nuclear well logging, nuclear geophysics equipment (e.g., for gamma-neutron logging), for detection of thermal neutrons, etc. (see, e.g., [1-18]). Indeed, this material has a high density (6.71 g/cm^3), high effective atomic number (Z=59), fast decay time (20-60 ns), large light yield (in some samples, up to 11500 photons/MeV [11] or 12500 photons/MeV [19]) which is about 20-25 % of that of NaI:Tl [1, 5, 20, 21] and considerably larger compared to $Bi_4Ge_3O_{12}$ (BGO) (8000-9000 photons/MeV (see, e.g., [15, 16]). It has energy resolution of 7.8 % (662 KeV, 1 cm^3 crystal) better than in BGO, short radiation length (1.38 cm), excellent radiation stability (up to 10^9 rad), high thermal stability (up to 200 ^{o}C), and the emission in the blue spectral region (see, e.g., [1, 5, 7, 10, 11, 19, 22]). Besides, GSO:Ce is relatively cheaper to produce as compared with Lu_2SiO_5:Ce (LSO:Ce), the best Ce^{3+}-doped oxyorthosilicate-based scintillation material and has no natural radioactivity. A much larger Ce concentration (C_{Ce}) can be achieved in GSO:Ce (up to 5 mol %) [5, 7] as compared with LSO. Both the light output and the scintillation decay time of GSO depend on C_{Ce}, reaching the best values at C_{Ce}=0.5-0.6 mol % (see, e.g., [1, 3, 5-7, 11-13, 17, 20-27]). Besides GSO, mixed $Lu_{2x}Gd_{2-2x}SiO_5$ crystals (with x varying from 0 to 1), which have even

more attractive scintillation characteristics, were also prepared and studied (see, e.g., [16, 28-35] and references therein). These crystals were denoted also as $(Lu,Gd)_2SiO_5$:Ce [30] (LGSO:Ce) crystals.

Thermally stimulated luminescence (TSL) of GSO:Ce crystals had been studied only in a few papers. The TSL glow curves were mainly measured with a heating rate of β=5 K/min for the integrated emission of the crystals X-ray irradiated at room temperature (RT). In [36, 37], a complex TSL peak, consisting of strongly overlapping unresolved components located at about 400 K, 425 K, 490 K, 550 K, was reported. In [38], the main peak was observed at 391 K, and much weaker peaks at 420 K, 490 K and 550 K. The first peak was shown to be characterized by the first-order kinetics. The corresponding trap depth E_t was of 1.16 eV and the frequency factor f_0, of 3.17 x 10^{14} s^{-1}. Like in the other Ce-doped oxyorthosilicates, this peak was ascribed to an electron trapped at an oxygen vacancy. In [39], a similar TSL glow curve was observed but the dominating peak was located at 373 K. In [40], the presence at the TSL glow curve of the main 463 K peak and weaker 543 K and 633 K peaks was reported. It was also shown that in GSO:Ce nanophosphors, the main peak is strongly reduced and shifted to lower temperatures (down to 365 K [39] or 433 K [40]).

After irradiation at 77 K, the TSL of GSO:Ce was studied only in [41, 42]. In [41], the peaks at 100 K, 145 K, and 350 K were observed at the TSL glow curve of X-ray irradiated crystals. The value of E_t=0.7 eV was obtained for the 350 K peak. After thermal annealing in vacuum, the intensities of all the peaks increased and a new peak appeared at 280 K. In [42], the most intense peak at 140 K and weaker peaks at about 180 K, 240 K, 300 K, 350 K, 390 K, 450 K, and 540 K were observed with β=0.2 K/s after γ-irradiation of GSO:Ce. The TSL glow curve of the X-ray irradiated at 10 K LGSO:Ce crystal, measured with β=0.16 K/s, was reported in [30]. Several strongly overlapping TSL peaks in the 20-150 K temperature range and the peak around 320 K were observed. The trap depth values E_t varied from 0.08 eV for the TSL peak located at about 50 K to 0.29 eV for the peak around 120 K. For the 320 K peak, E_t=0.51 eV. For the improved LGSO:Ce crystal X-ray irradiated at 80 K, two main peaks located at 110 K and 315 K were obtained in [31] with β=5 K/min.

Thus, very different information is reported in different papers on the positions and parameters of the TSL glow curve peaks in GSO:Ce and LGSO:Ce crystals. The TSL characteristics of the undoped GSO and LGSO crystals were not studied yet. In all the above-mentioned papers, the TSL glow curves were measured only for the integrated luminescence.

Like in other oxyorthosilicate crystals, in the X-ray irradiated GSO and LGSO crystals, the holes can be trapped at oxygen O^{2-} ions (see, e.g., [43]). Similar to aluminum garnets (see, e.g., [44]), in Ce^{3+}- and Tb^{3+}-containing GSO and LGSO crystals, the holes can be trapped also at the impurity Ce^{3+} and Tb^{3+} ions. The recombination of thermally released electrons with the O^--type, Ce^{4+} or Tb^{4+} hole centers is accompanied with the intrinsic, Ce^{3+} or Tb^{3+} emission, respectively. The electrons can be trapped at intrinsic crystal lattice defects (e.g., at oxygen vacancies [45-47]) as well as at impurity (e.g., Eu^{3+}) ions [44]. The recombination of thermally released holes with the electron Eu^{2+} centers is accompanied with the Eu^{3+} emission. Owing to that, the peaks of an electron origin should dominate at the TSL glow curves measured for the intrinsic and Tb^{3+}-, Ce^{3+}-related emission, while at the TSL glow curves measured for the Eu^{3+}-related emission, the peaks of a hole origin should dominate. The emission bands of the intrinsic, Ce^{3+}- , Tb^{3+}-related and Eu^{3+}-related luminescence centers are located in the 2.5-3.2 eV and 1.7-2.1 eV energy ranges, respectively (see, e.g., [32, 39, 46, 48-57]), i.e. they are well separated.

To identify the TSL peaks, arising from the thermal decay of electron and hole centers in GSO- and LGSO-based crystals, we have carried out a detailed and systematic study of the TSL characteristics for the Ce^{3+}-doped and the nominally undoped but Ce^{3+}-, Tb^{3+}-, and Eu^{3+}-contaminated GSO and LGSO single crystals X-ray irradiated at 80 K and at 4 K or 8 K. The

TSL glow curves are measured in the 4-520 K temperature range separately for the intrinsic, Ce^{3+}- or Tb^{3+}-related and for the Eu^{3+}-related emission bands. Besides, the TSL spectra are measured for each TSL glow curve peak and compared with the spectra of the X-ray excited luminescence, photoluminescence and afterglow. The thermal stability parameters (the trap depths E_t and the frequency factors f_0) are defined for the defects responsible for different TSL glow curve peaks. Due to a large nuclear spin of Gd, the electron paramagnetic resonance studies for these crystals are not possible. Therefore, the TSL method becomes especially important for investigation of electron and hole traps in these materials.

2. Experimental procedure

We have studied Ce^{3+}-doped Gd_2SiO_5 (GSO) and $(LuGd)_2SiO_5$ (LGSO) crystals, and the nominally undoped GSO and LGSO crystals. The Gd concentration in the LGSO and LGSO:Ce samples was 50 at. % related to the sum of lanthanides (Lu+Gd). Therefore, the formula of the LGSO crystals used in this paper can be written as $LuGdSiO_5$. All the crystals were grown under the same conditions in the Institute for Scintillation Materials, Kharkiv, Ukraine. The single crystals were growm by the Czochralski method in iridium crucibles under argon atmosphere with addition of oxygen up to 1.5 vol%. Powders of Lu_2O_3, Gd_2O_3, SiO_2, and CeO_2 with the purity not worse than 99.99 % mixed in stoichiometric ratio were taken as the starting materials for crystal growth. According to [58], the melting temperatures of GSO and LGSO are 1800 °C and 1890 °C, respectively. The GSO and GSO:Ce crystals were grown along the [100] direction. The LGSO and LGSO:Ce crystals were grown along the [210] direction. According to the XRD analysis, GSO belongs to the monoclinic $P2_1/c$ structure (a=9.127, b=7.051, c=6,743, V=413,831, β=107.519). The LGSO samples studied belong to the monoclinic C2/c structure (a=14.415, b=6.726, c=10.451, V=857.714, β=122.179). No admixtures of other phases were found. The typical size of the crystals was 30 mm in diameter and 50 mm in height. All the crystals were imposed to post-growth annealing at 1500 °C to prevent cracking at cutting and polishing. The Ce-doped crystals contained from 0.4 to 0.6 mol % of Ce. The nominally undoped crystal contained traces (few ppm) of Ce^{3+}, Eu^{3+}, and Tb^{3+} ions.

Photoluminescence characteristics of the crystals studied were measured in the 80-400 K temperature range at the setup, consisting of a deuterium lamp (DDS-400), two monochromators (SF-4 and SPM-1) and a photomultiplier tube (FEU-39 or FEU-79) connected to an amplifier and recorder. All the spectra were corrected for the spectral distribution of the excitation light, the transmission and dispersion of the monochromators and spectral sensitivity of the detectors.

The X-ray luminescence spectra were excited at 8 K or 80 K with a X-ray tube (with a W anode operated at 30kV, 15mA) and measured with a Andor Shamrock B - 303i spectrograph equipped with a CCD camera (Andor DU-401A-BV). These spectra were not corrected.

For the TSL studies, a crystal located in a nitrogen or helium cryostat was irradiated for 20 min by an X-ray source (with a Mo or W anode) operating at 50 kV or 30 kV and 15 mA. The TSL glow curves were measured in the 4-520 K temperature range separately for the intrinsic, Ce^{3+}- and/or Tb^{3+}-related emission and for the Eu^{3+}-related emission. In the 8-320 K range (in a closed cycle helium cryostat) and in the 4-300 K range (in a liquid helium cryostat), the heating rate was 0.1 K/s, the needed emission ranges were separated by a monochromator Andor Shamrock B - 303i or by the optical filters (ZhS-4+FS-7, KS-14, or UFS-6 with the transmittance in the 3.0-3.5 eV, E<2.0 eV, and 3.25-3.85 eV energy ranges, respectively). The TSL intensity was detected with a CCD camera (Andor DU-401A-BV) or a photon counting head Hamamatsu H8259. For the TSL glow curves measurement in the 80-520 K range (in a

vacuum nitrogen cryostat), the heating rate was 0.2 K/s, the needed emission ranges (E_{em}=2.95-3.20 eV or E_{em}=1.85-2.00 eV) were separated by the monochromator SPM-1, and the TSL intensity was detected by a photomultiplier tube (FEU-39 or FEU-79) connected to an amplifier and recorder. The TSL glow curves were not corrected for the temperature dependences of the corresponding emissions intensity. The TSL spectra were measured with the use of the Andor Shamrock B - 303i spectrograph equipped with a CCD camera (Andor DU-401A-BV) and were not corrected either. At the same experimental conditions, the TSL of the non-irradiated crystals was not detectable.

3. Experimental results and discussion

3.1. The nominally undoped and Ce-doped GSO crystals

In the photoluminescence spectrum of ***the nominally undoped GSO crystal*** measured at 80 K, a broad intrinsic emission band located at about 2.55 eV considerably dominates. Additionally, the emission bands located in the 2.5-3.3 eV and 1.7-2.1 eV energy ranges are present (Fig. 1(a), solid line). The bands in the 2.5-3.3 eV range arise from the traces of Tb^{3+} and Ce^{3+} ions. The comparison of the emission spectra of different rare-earth ions in GSO allows us to conclude that the Eu^{3+} emission dominates in the 1.7-2.1 eV energy range (see, e.g., [57]). Indeed, as the Tb^{3+} content in the crystals studied is very small (few ppm), the emission bands in the 1.7-2.1 eV energy range cannot arise from Tb^{3+} ions [55, 56]. These bands cannot arise also from Pr^{3+} ions, having the 4f – 4f luminescence at about 2.03-2.05 eV, as no ultraviolet (4.42 eV) emission of Pr^{3+}, arising from the 5d – 4f transitions (see, e.g., [59]) is observed. Consequently, Pr^{3+} ions are absent in the crystals studied. In principle, the emission in this energy range can arise also from Sm^{3+} ions (see, e.g., [46]). Also a GSO:Dy crystal has two complex emission bands of comparable intensities located around 2.57 eV and in the 2.12-2.17 eV energy range [60]. However, the former band is not observed in our GSO crystal, which means that Dy^{3+} ions are absent. Besides, both the Sm^{3+} and Dy^{3+} ions can trap electrons, like Eu^{3+} ions [44], i.e., the corresponding emission bands, if present, should also appear in the hole recombination processes. The emission around 2.0 eV in GSO crystal cannot arise from Gd^{3+} ions as well [61]. Due to the wide monochromator slits used at the measurement of the photoluminescence spectrum presented in Fig. 1a, the structure of the Tb^{3+}-, Ce^{3+}, and Eu^{3+}-related emission bands is not evident. In the X-ray excited luminescence spectrum, the more intense red (most probably, Eu^{3+}-related) emission and weaker intrinsic 2.55 eV emission are mainly observed (dotted line).

At the TSL glow curves of the X-ray irradiated at 80 K GSO crystal (Fig. 2(a)) measured for the intrinsic and Tb^{3+}-, Ce^{3+}-related emission (with E_{em}=3.1 eV) (solid line) and for the Eu^{3+}-related emission (with E_{em}=1.85 eV) (dashed line), the main peaks are observed at about 107 K, 145 K and 336 K (see Table 1). All the TSL peaks are of complex structure. The relative intensities of these peaks depend on the emission energy. At the TSL glow curve measured for the 3.1 eV emission, the peak at 107 K dominates over the 145 K peak and, especially, over the complex 336 K peak, and an additional peak appears at 376 K. At the TSL curve measured for the 1.85 eV emission, the peak at 333 K is a dominating one and the 145 K peak is more intense as compared with the 107 K peak. Much weaker peaks are observed around 167 K, 207 K, 244 K, 397 K, 436 K, and 470 K. After irradiation of the GSO crystal at 8 K (Fig. 3(a)), additional TSL peaks located at about 56 K, 80 K and 88 K appear. The relative intensities of these peaks measured for the intrinsic emission (with E_{em}=2.75 eV) (solid line) and for the Eu^{3+}-related emission (with E_{em}=2.03 eV) (dashed line) are comparable.

However, in the latter case, the relative intensities of the higher-temperature peaks, located at about 111 K, 153 K, 209 K, and 248 K, are noticeably larger as compared with the former case.

In the afterglow spectrum of the GSO crystal measured at 8 K, the intrinsic emission dominates over the Eu^{3+}-related emission (Fig. 4(a), curve 1), while in the TSL spectra of this crystal, the Eu^{3+}-related emission bands dominate in all the TSL peaks, especially at T>100 K (curves 2-5). The relative intensity of the intrinsic 2.55 eV emission, which is suggested to arise from the recombination of electrons with the holes trapped at oxygen ions, is especially large in the TSL peaks located at T<100 K. The above-mentioned effects can be partly caused by a stronger thermal quenching of this emission as compared with the Eu^{3+} emission (see the inset in Fig. 1(b)).

The data obtained during the study of the nominally undoped GSO crystal indicate that the observed TSL peaks consist of strongly overlapping electron and hole components whose relative contributions depend on the temperature. The TSL peaks located in the T<100 K temperature range are mainly of an electron origin. The peaks located in the 110-250 K range and at about 397 K, 436 K, 470 K (shown in bold in Table 1) can contain also the hole components arising from the recombination of thermally released holes with the electron Eu^{2+} centers.

From the TSL data, the parameters of the traps (trap depths E_t and frequency factors f_0) corresponding to each TSL can be defined. The E_t values are obtained by the well-known partial cleaning method (for more details, see, e.g., [46] and references therein) from the slope of the $\ln I_{TSL}(1/T)$ dependences after heating of the irradiated sample up to the selected temperatures T_{stop}. For the GSO crystal irradiated at 80 K, the dependences of the E_t values on T_{stop}, obtained from the analysis of the TSL glow curves measured for the most intense Eu^{3+}-related emission, are presented in Fig. 5(a). In the case of the first-order recombination kinetics, the frequency factors f_0 can be calculated with the use of the expression

$$f_0=(\beta E_t / kT_m^2) \exp (E_t / kT_m),$$

where β is the crystal heating rate, k is the Boltzmann factor, and T_m is the maximum position of the considered peak at the TSL glow curve. By analogy with other oxyorthosilicates (see, e.g., [62] and references therein) and based on the data obtained in [38], the first-order recombination kinetics is suggested for all the TSL peaks in GSO. Due to a strong overlap of the TSL peaks, only approximate values of the E_t and f_0 parameters could be obtained. The T_m value for each peak is obtained from the partial cleaning data by the method similar to that described in [63]. Namely, T_m is taken as the temperature where the peak position becomes independent of T_{stop}. According to our estimations, T_m values for the main TSL peaks can be defined with an accuracy of about 2-5 K. The values of E_t are defined with an accuracy of about 5-10 %. For the f_0 values, only an order of magnitude can be shown.

In the photoluminescence spectrum ***of the GSO:Ce crystal*** measured at 80 K (Fig. 1(b)), the Ce^{3+}-related Ce1 (solid line) and Ce2 (dashed line) emission bands are mainly observed. These bands arise from the Ce^{3+} ions substituting for Gd^{3+} ions located in two different GSO crystal lattice sites (1 and 2). The Ce1 emission strongly dominates in both the photoluminescence and the X-ray excited (dotted line) luminescence spectra. The latter spectrum contains also the Ce2 and intrinsic emission bands.

The TSL glow curves measured for the Ce^{3+} emission in different GSO:Ce crystals are found to be different. This indicates to the different origin and concentration of intrinsic electron traps in these crystals. The TSL glow curves of GSO:Ce are independent of the emission energy and are similar to those published in [41, 42]. After X-ray irradiation at 80 K, the complex peaks located at about 107 K, 140 K, 165 K, 214 K, 248 K, 285 K, 365 K, 400 K, and 462 K are observed (see Fig. 2(b) and Table 1). As it was mentioned above, the centers

responsible for the lowest-temperature peak can be partly destroyed during the irradiation at 80 K. As compared with the 140 K peak, the intensity of the 365 K peak is about 6 times smaller, the intensities of the peaks at 165 K, 400 K and 462 K are about 27 times smaller, and the other peaks are very weak. Relative intensities of the higher-temperature TSL peaks can be reduced due to the thermal quenching of the Ce1 emission (see the inset in Fig. 1(b)). After X-ray irradiation of this crystal at 8 K, additional intense complex peaks located at 37 K, 45 K, 63 K, and 72 K appear (Fig. 3(b)). The intensities of the 107 K and 146 K peaks are comparable. In the spectrum of afterglow (Fig. 4(b), curve 1) and in all the TSL peaks (curves 2-5), mainly the Ce^{3+}-related Ce1 emission is observed.

At the TSL glow curve of GSO:Ce, the peaks of an electron origin, which arise from the recombination of electrons with the hole Ce^{4+} centers, considerably dominate. The dependences of the E_t values on T_{stop} obtained for the GSO:Ce crystal X-ray irradiated at 80 K are presented in Fig. 5(b). From the comparison of Fig. 5(b) with Fig. 5(a), it is evident that for closely located TSL peaks, the E_t values in Fig. 5(a) are smaller as compared with Fig. 5(b). The approximate values of the E_t and f_0 parameters obtained for different TSL peaks are shown in Table 1. From the comparison of the parameters obtained for the thermally stimulated intrinsic, Tb^{3+}- and Ce^{3+}-related emissions in the GSO and GSO:Ce crystals and Eu^{3+}-related emission in the GSO crystal, we can conclude that the values of thermal stability parameters for hole traps are smaller as compared with those of electron traps. A similar result was obtained for hole-related TSL peaks in [62].

3.2. The nominally undoped and Ce-doped LGSO crystals

In both the photoluminescence spectrum (Fig. 6(a), solid line) and X-ray excited luminescence spectum (dotted line) of ***the nominally undoped LGSO crystal,*** the emission bands, arising mainly from Gd^{3+} (at 3.92 eV) and Tb^{3+} (in the 2.7-3.3 eV range) ions are evident. The bands located around 2.55 eV and 2.15 eV can arise from Dy^{3+} ions [60], and the bands in the 1.7-2.1 eV range are suggested to arise mainly from Eu^{3+} ions [57]. Indeed, as it is mentioned in the item 3.1, the latter bands cannot arise neither from Tb^{3+} ions [55, 56], nor from Pr^{3+} [59] or Gd^{3+} [61] ions. As both the Eu^{3+} and Dy^{3+} ions can trap electrons [44], the emission in the 1.7-2.1 eV energy range should accompany the hole recombination processes. Under excitation in the Gd^{3+}-related 4.5 eV absorption band, these emissions appear due to the energy transfer from Gd^{3+} ions.

The TSL glow curves, measured mainly for the Tb^{3+}-related emission (with E_{em}=3.2 eV) and for the Eu^{3+}-related emission (with E_{em}=1.85 eV) after X-ray irradiation of the crystal at 80 K, are strongly different (Fig. 7(a)). Unlike the case of the GSO and GSO:Ce crystals, this difference cannot arise from different temperature dependences of the Tb^{3+}- and Eu^{3+}-related emissions. Indeed, as it is evident from the inset in Fig. 6(a), the temperature dependences of their intensities I(T) are similar. Under 4.5 eV excitation, the intensities of both the Eu^{3+}- (curve 1) and the Tb^{3+}- (curve 2) related emission decrease about twice as the temperature increases from 80 K to 230 K and then remains constant. The same I(T) dependence is observed under the 4.5 eV excitation for the Gd^{3+}-related 3.92 eV emission (curve 3). The TSL glow curves measured after X-ray irradiation at 4 K are shown in Fig. 8(a). From the TSL spectra measured for different TSL peaks (Fig. 9(a)), it is seen that in the T<110 K temperature range and in the peak located at 333 K, the Tb^{3+}-related emission bands dominate. In the 160-290 K temperature range, mainly the Eu^{3+}-related emission is thermally stimulated. These data allow us to conclude that the former TSL peaks are mainly of an electron origin and arise from the recombination of thermally released electrons with the hole Tb^{4+} centers. The peaks located in the 160-290 K range (shown in bold in Table 2) should mainly be of a hole origin and most probably arise from the recombination of the thermally released holes with the electron Eu^{2+}

centers. Thus, in this crystal, the TSL peaks of electron and hole origin can be clearly separated.

The dependences of the trap depth values E_t on the temperature T_{stop}, obtained by the partial cleaning method from the TSL curves measured separately for the Tb^{3+}-related emission and the Eu^{3+}-related emission of the LGSO crystal X-ray irradiated at 80 K, are shown in Fig. 10(a). The approximate values of the trap depths E_t and frequency factors f_0 corresponding to each TSL peak are presented in Table 2. Again, smaller values of E_t and f_0 are obtained for the hole centers as compared with the electron centers. The smaller E_t and f_0 values obtained for the TSL peak around 100 K at the TSL glow curve measured for the Eu^{3+} emission can indicate that this peak contains also a hole component.

In the photoluminescence spectrum of ***LGSO:Ce*** (see, e.g., Fig. 6(b)), the Ce^{3+}-related Ce1 (solid line) and Ce2 (dashed line) emission bands are mainly observed. The Ce1 emission strongly dominates in both the photoluminescence and the X-ray excited (dotted line) luminescence spectra. Besides the Ce^{3+}-related emissions, weak emission bands located in the 1.7-2.1 eV energy range (empty circles) and around 3.75 eV (filled circles) are also observed. They are assumed to arise from Eu^{3+} ions and some unidentified defects, respectively. A weak emission band peaking in the 3.7-3.8 eV energy range exists in all the crystals studied. In the Ce-doped crystals, this emission band is strongly distorted by the intense Ce^{3+}-related absorption band located around 3.5-3.6 eV.

At the TSL glow curve measured for the Ce^{3+} emission (Fig. 7(b)), two main peaks, located at 107 K and 319 K, and much weaker peaks, located at ≈162 K and 382 K, are observed after X-ray irradiation at 80 K. In the experiments with the partial cleaning, a complex structure of the TSL peaks appears. Namely, the complex 319 K peak can consist of a stronger 317-318 K component and weaker components located at about 330 K and 340 K. After irradiation at 4 K, the main TSL peak is located at about 91 K and much weaker peaks, in the 115-250 K range (Fig. 8(b)).

The comparison of the data obtained at the study of the nominally undoped and Ce^{3+}-doped LGSO crystals allows us to conclude that the TSL peaks at 107 K and ≈318 K are of an electron origin, and the peaks located at 115 K, 159-165 K, and 204 K are mainly of a hole origin. It is interesting to note that mainly the latter peaks and a weak peak at 35 K appear at the TSL glow curve measured for the ≈3.75 eV emission (Fig. 8(b), dotted line). However, this effect is observed only in the case when before the irradiation, the previously irradiated crystal was heated only up to 300 K, i.e., the most effective hole traps (Ce^{3+} ions) are filled by holes. This indicates that at T<300 K the holes are mainly trapped at oxygen ions, and the above-mentioned TSL peaks arise from various O^--type hole centers.

The approximate values of the trap depths E_t and frequency factors f_0 obtained for LGSO:Ce are presented in Fig. 10(b) and Table 2. Different positions of the main low-temperature (around 100 K) peak in Fig. 7(b) and Fig. 8(b) as well as different E_t values obtained from these experiments indicate its complex structure. We suggest that after irradiation at 80 K mainly the higher-temperature component of this peak appears.

At the TSL glow curves of some compounds, besides discrete glow peaks, broad bands are present. These bands have been ascribed to thermally assisted tunnelling processes (see, e.g., [46]) or quasi-continuous distributions of trapping levels [64, 65]. Although the TSL glow curves of the crystals studied can be considered as the superpositions of the overlapping individual TSL peaks, the contribution of the above-mentioned features to the TSL intensity needs further investigations. These investigations can be carried out by the T_{max} - T_{stop} method, which has been proposed in [63] and successfully used recently in [64-65] for the determination of the number and positions of TSL peaks as well as of the E_t and f_0 values corresponding to each peak. We hope that further studies will allow us to obtain preciser values

of thermal stability parameters for various electron and hole traps in GSO- and LGSO-based crystals.

4. Conclusions

The TSL glow curves, measured for the intrinsic, Tb^{3+}- or Ce^{3+}-related emission and for the Eu^{3+}-related emission of Gd_2SiO_5 and $LuGdSiO_5$ crystals, are found to be different. From the analysis of these TSL glow curves and the TSL spectra corresponding to each TSL peak, the electron or hole origin of the TSL peaks is identified. The intense complex peaks located in the 30-100 K and 320-365 K temperature ranges are mainly of an electron origin. They are suggested to arise from the thermal release of the electrons trapped at various oxygen-vacancy-related defects and their subsequent recombination with the hole O^--type, Tb^{4+}, or Ce^{4+} centers accompanied with the intrinsic, Tb^{3+}-, or Ce^{3+}-related emission, respectively. The complex TSL glow curve peaks located mainly in the 115-300 K temperature range contain the peaks of a hole origin. The lower-temperature peaks are suggested to arise from the thermal release of the holes, trapped at the regular oxygen ions (self-trapped holes). The higher-temperature peaks can arise from the holes trapped at the oxygen ions located close to some intrinsic or impurity crystal lattice defects. The subsequent recombination of the released holes with the electron Eu^{2+} centers is accompanied with the Eu^{3+}-related emission. The electron and hole centers of similar origin have been recently detected in single crystals of yttrium and lutetium oxyorthosilicates by the EPR [43] and TSL [61] methods. The values of thermal stability parameters (the trap depths E_t and especially the frequency factors f_0) for the hole traps are found to be considerably smaller as compared with the parameters characteristic for the electron traps. This fact can be used for identification of the origin of the traps corresponding to TSL peaks in various materials.

Acknowledgements

The work was supported by the Estonian Research Council – Institutional Research Funding IUT02-26, the project No. 8678 of the Estonian Science Foundations, the NATO project CBP.NUKR.CLG984305, and the Latvian Science Council grant 302/2012.

References

[1] K. Takagi, T. Fukazawa, Appl. Phys. Lett. 42 (1983) 43.
[2] L. Eriksson, M. Bergstrom, C. Rohm, S. Holte, M. Kesselberg, J. Litton, IEEE Trans. Nucl. Sci. 33 (1986) 446.
[3] H. Ishibashi, K. Shimizu, K. Susa, S. Kubota, IEEE Trans. Nucl. Sci. 36 (1989) 170.
[4] A. Lempicki, J. Glodo, Nucl. Instrum. Methods Phys. Res. A 416 (1989) 333.
[5] C.L. Melcher, J.S. Schweitzer, T. Utsu, S. Akiyama, IEEE Trans. Nucl. Sci. 37 (1990) 161.
[6] H. Ishibashi, Nucl. Instrum. Methods Phys. Res. A 294 (1990) 271.
[7] C.L. Melcher, J.S. Schweitzer, R.A. Manente, C.A. Peterson, IEEE Trans. Nucl. Sci. 38 (1991) 506.
[8] M. Kobayashi, K. Takamatsu, S. Ide, K. Mori, S. Sugimoto, H. Takaki, M. Yuasa, M. Ishii, Nucl. Instrum. Methods Phys. Res. A 306 (1991) 139.
[9] P. Lecoq, M. Schussler, M. Schneegans, Nucl. Instrum. Methods Phys. Res. A 315 (1992) 337.

[10] B.A. Roscoe, J.A. Grau, R.A. Manente, C.L. Melcher, C.A. Peterson, J.S. Schweitzer, C. Stoller, IEEE Trans. Nucl. Sci. 39 (1992) 1412.
[11] P.L. Reeder, Nucl. Instrum. Methods Phys. Res. A 340 (1994) 371.
[12] P.A. Rodnyi, Physical Processes in Inorganic Scintillators, CRC Press, Boca Raton, 1997.
[13] M. Tanaka, K. Hara, S. Kim, K. Kondo, H. Takano, M. Kobayashi, H. Ishibashi, K. Kurashige, K. Susa, M. Ishii, Nucl. Instrum. Methods Phys. Res. A 404 (1998) 283.
[14] S. Surti, J.S. Karp, R. Friefelder, F. Liu, IEEE Trans. Nucl. Sci. 47 (2000) 1030.
[15] C.W.E. van Eijk, Phys. Med. Biol. 47 (2002) R85; Nucl. Instrum. Methods Phys. Res. A 509 (2003) 17.
[16] J.L. Humm, A. Rosenfeld, A. Del Cuerra, Eur. J. Nucl. Med. Mol. Imaging 30 (2003) 1574.
[17] P. Lecoq, A. Annenkov, A. Gektin, M. Korzhik, C. Pedrini, Inorganic Scintillators for Detection Systems, Springer-Verlag, Berlin, 2006.
[18] R. Lecomte, Eur. J. Nucl. Med. Mol. Imaging 36 (2009) 69.
[19] C.L. Melcher, J.S. Schweitzer, C.A. Peterson, R.A. Manente, H.Suzuki, Proc. Int. Conf. on Inorganic Scintillators and their Applications (SCINT'95), eds. P. Dorenbos, C.W.E. van Eijk, Delft Univ. Press, The Netherlands, 1996, pp. 309-316.
[20] H. Suzuki, T.A. Tombrello, C.L. Melcher, J.S. Schweitzer, Nucl. Instrum. Methods Phys. Res. A 320 (1992) 263.
[21] H. Suzuki, T.A. Tombrello, C.L. Melcher, C.A. Peterson, J.S. Schweitzer, Nucl. Instrum. Methods Phys. Res. A 346 (1994) 510.
[22] H. Ishibashi, K. Kurashige, Y. Kurata, K. Susa, M. Kobayashi, M. Tanaka, K. Hara, M. Ishii, IEEE Trans. Nucl. Sci. 45 (1998) 518.
[23] M. Sekita, Y. Miyazawa, T. Akahane, T. Chiba, J. Appl. Phys. 66 (1989) 373.
[24] M. Kobayashi, M. Ishii, Nucl. Instrum. Methods Phys. Res. B 61 (1991) 491.
[25] M. Kobayashi, M. Ieiri, K. Kondo, T. Miura, H. Noumi, M. Numajiri, Y. Oki, T. Suzuki, M. Takasaki, Y. Yamanoi, Nucl. Instrum. Methods Phys. Res. A 330 (1993) 115.
[26] V.G. Baryshevskii, D.M. Kondratiev, M.V. Korzhik, V.B. Pavlenko, A.A. Fedorov, J. Lumin. 60/61 (1994) 956.
[27] D.M. Kondratiev, M.V. Korzhik, A.A. Fedorov, V.B. Pavlenko, Phys. Status Solidi B 197 (1996) 251.
[28] S. Akiyama, H. Ishibashi, T. Utsu, C.L.Melcher, U.S. Patent 5 (1993) 264, 154.
[29] G.B. Loutts, A.I. Zagumenni, S.V. Lavrishichev, Yu.D. Zavartsev, P.A. Studenikin, J. Cryst. Growth 174 (1997) 331.
[30] P. Szupryczynski, C.L. Melcher, M.A. Spurrier, M.P. Maskarinec, A.A. Carey, A.J. Wojtowicz, W. Drozdowski, D. Wisniewski, R. Nutt, IEEE Trans. Nucl. Sci. 51 (2004) 1103.
[31] O. Sidletskiy, V. Bondar, B. Grinyov, D. Kurtsev, V. Baumer, K. Belikov, K. Katrunov, N. Starzhinsky, O. Tarasenko, V. Tarasov, O. Zelenskaya, J. Crystal Growth, 312 (2010) 601.
[32] I.A. Kamenskikh, A.N. Belsky, A.V. Gektin, M.V. Limonova, S. Neicheva, O. Sidletskiy, IEEE Trans. Nucl. Sci. 61 (2014) 290.
[33] S. Yamamoto, Radioisotops 47 (1998) 673.
[34] M. Kapusta, M. Moszynski, M. Balcerzyk, J. Braziewicz, D.Wolski, J. Pawelke, W. Klamra, IEEE Trans. Nucl. Sci. 47 (2000) 1341.
[35] B.J. Pichler, G. Böning, M. Rafecas, M. Schlosshauer, E. Lorenz, S.I. Ziegler, IEEE Trans. Nucl. Sci. 46 (1999) 289.
[36] D.W. Cooke, B.L. Bennett, R.E. Muenchausen, K.J. McClellan, J.M. Roper, M.T. Whittaker, J. Appl. Phys. 86 (1999) 5308.

[37] D.W. Cooke, B.L. Bennett, K.J. McClellan, J.M. Roper, M.T. Whittaker, J. Lumin. 92 (2001) 83.
[38] D.W. Cooke, B.L. Bennett, K.J. McClellan, J.M. Roper, Radiat. Measur. 33 (2001) 403.
[39] E.G. Yukihara, L.G. Jacobsohn, M.W. Blair, B.L. Bennett, S.C. Tornga, R.E. Muenchausen, J. Lumin. 130 (2010) 2309.
[40] L.G. Jacobsohn, S.C. Tornga, M.W. Blair, B.L. Bennett, R.E. Muenchausen, R. Wang, P.A. Crosier, D.W. Cooke, J. Appl. Phys. 110 (2011) 083515.
[41] L. Nagornaja, N. Starzhinkiy, K. Katrunov, B. Grinyov, E. Loseva, V. Ryzhikov, G. Onishchenko, Proc. of the Eigth Int. Conf. on Inorganic Scintillators and their Use in Scientific and Industrial Applications, Alushta, Ukraine, September 19-23, 2005, pp. 181-184.
[42] A.F. Rakov, U.S. Salikbaev, A.K. Islamov, R.H. Bartram, C.L. Melcher, J. Lumin. 130 (2010) 2004.
[43] V.V. Laguta, M. Nikl, Phys. Status Solidi B 250 (2013) 254.
[44] P. Dorenbos, J. Lumin. 134 (2013) 310.
[45] P. Dorenbos, C.W.E. van Eijk, A.J.J. Bos, C.L. Melcher, J. Phys.: Condens. Matter 6 (1994) 4167.
[46] A. Vedda, M. Nikl, M. Fasoli, E. Mihokova, J. Peichal, M. Dusek, G. Ren, C.R. Stanek, K.J. McClellan, D.D. Byler, Phys. Rev. B 78 (2008) 195123.
[47] R. Visser, C.L. Melcher, J.S. Schweizer, H. Suzuki, T.A. Tombrello, IEEE Trans. Nucl. Sci. 41 (1994) 689.
[48] H. Suzuki, T.A. Tombrello, C.L. Melcher, J.S. Schweitzer, Nucl. Instrum. Methods Phys. Res. A 320 (1992) 263.
[49] H. Suzuki, T.A. Tombrello, C.L. Melcher, J.S. Schweitzer, IEEE Trans. Nucl. Sci. 40 (1993) 380.
[50] C.L. Melcher, M. Schmand, M. Eriksson, L. Eriksson, M. Casey, R. Nutt, J.L. Lefaucheur, B. Chai, IEEE Trans. Nucl. Sci. 47 (2000) 965.
[51] D.W. Cooke, K.J. McClellan, B.L. Bennett, J.M. Roper, M.T. Whittaker, R.E. Muenchausen, R.C. Sze, J. Appl. Phys. 88 (2000) 7360.
[52] G. Ren, L. Qin, S. Lu, H. Li, Nucl. Instrum. Methods Phys. Res. A 531 (2004) 560.
[53] W. Drozdowski, A. Wojtowicz, D. Wisniewski, P. Szupryczynski, S. Janus, J.-L. Lefaucheur, Zh. Gou, J. Alloys & Compounds 380 (2004) 146.
[54] D.W. Cooke, R.E. Muenchausen K.J. McClellan, B.L. Bennett, Optical Materials 27 (2005) 1781.
[55] P.C. Ricci, C.M. Carbonaro, R. Corpino, C. Cannas, M. Salis, J. Phys. Chem. C 115 (2011) 16630.
[56] M. Salis, C.M. Carbonaro, R. Corpino, A. Anedda, P.C. Ricci, J. Phys.: Condens. Matter 24 (2012) 295401.
[57] Y. Chen, B. Liu, C. Shi, M. Kirm, M. True, S. Vielhauer, G. Zimmerer, J. Phys.: Condens. Matter 17 (2005) 1217.
[58] M. Glowacki. G. Dominiak-Dzik, W. Ryba-Romanowski, R. Lisiecki, A. Strzep, T. Runka, M. Drozdowski, V. Domukhovski, R. Diduszko, M. Berkowski, J. of Solid State Chemistry 186 (2012) 268.
[59] J. Peichal, M. Nikl, E. Mihokova, J.A. Mares, A. Yoshikawa, H. Ogino, K.M. Schillemat, A. Krasnikov, A. Vedda, K. Nejezchleb, V. Mucka, J. Phys. D: Appl. Phys. 42 (2009) 055117.
[60] R. Lisiecki, G. G. Dominiak-Dzik, P. Solarz, W. Ryba-Romanowski, M. Berkowski, M. Glowacki, Appl. Phys. B 98 (2010) 337.
[61] K. Mori, M. Nakayama, H. Nishimura, Phys. Rev. B 67 (2003) 165206.
[62] T. Kärner, V.V. Laguta, M. Nikl, S. Zazubovich, Phys. Status Solidi B, 251 (2014) 741.
[63] S.W.S. McKeever, Phys. Status Solidi A 62 (1980) 331.

[64]W. Drozdowski, K. Brylew, S.M. Kaczmarek, D. Piwowarska, Y. Nakai, T. Tsuboi, W. Huang, Radiat. Measur. 63 (2014) 26.
[65] K. Brylew, W. Drozdowski, A.J. Wojtowicz, K. Kamada, A. Yoshikawa, J. Lumin. 154 (2014) 452.

Table 1. Parameters of the traps (the TSL peak maximum T_m, trap depth E_t, frequency factor f_0) associated with different peaks at the TSL glow curves measured for the intrinsic, Ce^{3+}-, Tb^{3+}-, and Eu^{3+}-related emissions of various GSO-based crystals X-ray irradiated at 8 K and 80 K. The first numbers are obtained in the helium cryostat (with β=0.1 K/s), and the second ones, in the nitrogen cryostat (with β=0.2 K/s). The parameters of hole traps are shown in bold.

Crystal	Emission	T_m, K		E_t,eV		f_0, s^{-1}
GSO	Intrinsic; Tb^{3+}; Ce^{3+}	55				
		79				
		86				
		108	107			
		149	145			
		165	165			
		207	202			
		250	246			
			336			
			376			
			430			
	Eu^{3+}	57		0.04		
		82		0.12		$6x10^5$
		89		0.15		$7x10^6$
		111	108	0.18	0.26	$3x10^6$; $7x10^{10}$
		153	**145**	**0.31**	**0.36**	**$3x10^8$; 10^{11}**
		164	**167**		**0.38**	**10^{10}**
		209	**207**		**0.40**	**10^8**
		248	**244**		**0.52**	**10^9**
			333		0.95	$5x10^{12}$
			397		-	-
			436		**1.30**	**$2x10^{13}$**
			470		**1.45**	**$6x10^{13}$**
GSO:Ce	Ce^{3+}	37				
		45		0.02		
		63		0.05		
		72		0.11		10^6
		107	107	0.21	0.25	$2x10^8$; $3x10^{10}$
		146	140		0.42	$7x10^{13}$
		170	165		0.48	$2x10^{13}$
			200		-	-
			214		-	-
			248		-	-
			285		0.78-0.83	10^{12}-10^{13}
			365		1.14	10^{14}
			400		-	-
			462		-	-

Table 2. Parameters of the traps (the TSL peak maximum T_m, trap depth E_t, frequency factor f_0) associated with different peaks at the TSL glow curves measured for the Ce^{3+}-, Tb^{3+}-, and Eu^{3+}-related emissions of various LGSO-based crystals X-ray irradiated at 4 K and 80 K. The first numbers are obtained in the helium cryostat (with β=0.1 K/s), the second ones, in the nitrogen cryostat (with β=0.2 K/s). The parameters of hole traps are shown in bold.

Crystal	Emission	T_m, K		E_t,eV		f_0, s^{-1}
LGSO	Tb^{3+}	55		0.10		$6x10^7$
		75		0.17-0.20		10^{10}-10^{12}
		98		0.32		10^{15}
			113		0.38	10^{15}
		185	183	0.42	0.45	$4x10^9$-$4x10^{10}$
		280	277	0.75	0.80	$4x10^{11}$-10^{13}
			333		0.95;1.08	$5x10^{12}$; $5x10^{14}$
			387		1.25	$4x10^{14}$
			452		1.5	10^{15}
			490		-	-
	Eu^{3+}	55		0.09		$6x10^6$
		75		0.17		10^{10}
		100		**0.22**		**$3x10^9$**
			117		0.28	$5x10^{10}$
		165	**167**	**0.31**	**0.35**	**$4x10^7$; 10^9**
		230	**233**	**0.42**	**0.43**	**$(2-4)x10^7$**
		280	**290**	**0.57**	**0.60**	**$(2-5)x10^8$**
			330		0.95	10^{13}
			387		1.3	$2x10^{15}$
			455		-	-
LGSO:Ce	Ce^{3+}	91		0.26		10^{13}
			107		0.37	$6x10^{15}$
		163	162	0.48		$2x10^{13}$
			280		0.82	$2x10^{13}$
			318		0.91	$6x10^{12}$
			382		-	-
	Eu^{3+}	**35**		-		-
		92		0.27		10^{13}
			107		0.35	$2x10^{15}$
		115		-		-
		165	**163**	**0.33**		**$3x10^9$**
		204		-		-
			319		0.93	10^{13}
			382		-	-
	3.7 eV	**35**		-		-
		115		**0.23**		**$2x10^8$**
		159		**0.36-0.37**		**$(4-7)x10^9$**
		204		**0.42**		**$3x10^8$**

Highlights

X-ray irradiated undoped and Ce^{3+}-doped Gd_2SiO_5 and $LuGdSiO_5$ crystals are studied.
Thermally stimulated luminescence (TSL) characteristics are studied at 4-520 K.
TSL glow curves are measured for electron and hole recombination luminescence.
TSL glow curve peaks arising from various electron and hole centers are identified.
The origin and thermal stability parameters of electron and hole traps are defined.

Figure captions

Fig. 1. Normalized photoluminescence spectra of the (a) nominally undoped GSO and (b) GSO:Ce crystals measured at 80 K under excitation with E_{exc}=4.5 eV (a), E_{exc}=3.6 eV (b, solid line), and E_{exc}=3.2 eV (b, dashed line). The X-ray excited luminescence spectra measured at 8 K are shown in Figs. 1a and 1b by dotted lines. In the inset of Fig. 1b, temperature dependences of the intensities of the intrinsic (curve 1), Ce1- (curve 2) and Eu^{3+}-related (curve 3) emissions.

Fig. 2. Normalized (at 107 K) TSL glow curves measured after X-ray irradiation at 80 K of the (a) nominally undoped GSO crystal and (b) GSO:Ce crystal for the intrinsic, Tb^{3+}-, Ce^{3+}-related emission (with E_{em}=3.1 eV) (solid lines) and the Eu^{3+}-related emission (with E_{em}=1.85 eV) (dashed line).

Fig. 3. Normalized (at ≈88 K) TSL glow curves measured after X-ray irradiation at 8 K of the (a) nominally undoped GSO crystal and (b) GSO:Ce crystal for the intrinsic or Ce^{3+}-related emissions (E_{em}=2.75 eV or E_{em}=2.9 eV, respectively, solid lines) and for the Eu^{3+}-related emission (E_{em}=2.03 eV, dashed line).

Fig. 4. Afterglow (curve 1) and TSL (curves 2-5) spectra measured for the (a) nominally undoped GSO crystal and (b) GSO:Ce crystal at different temperatures shown in the legends. In Fig. 4a, the spectra are normalized in the maximum of the Eu^{3+}-related 2.03 eV emission band, and in Fig. 4b, in the maximum of the Ce^{3+}-related emission band.

Fig. 5. Dependences of E_t values on the temperature T_{stop} obtained from the analysis of the TSL glow curves measured (a) for the Eu^{3+} (E_{em}=1.85 eV) emission of the nominally undoped GSO crystal and (b) for the Ce^{3+} (E_{em}=2.95 eV) emission of the GSO:Ce crystal X-ray irradiated at 80 K. The average values of E_t and frequency factors f_0 are shown in Table 1.

Fig. 6. Photoluminescence spectra of the (a) nominally undoped LGSO crystal and (b) LGSO:Ce crystal measured at 80 K under E_{exc}=4.5 eV (a), E_{exc}=3.5 eV (b, solid line), and E_{exc}=3.8 eV (b, dashed line); the emission spectra of LGSO:Ce measured under E_{exc}=2.8 eV (b, empty circles) and E_{exc}=4.5 eV (b, filled circles). The X-ray excited luminescence spectra measured at 8 K (Figs. 6a and 6b, dotted lines; in Fig. 6a, the emission intensity in the E>2.7 eV range is increased 10 times). In the inset of Fig. 6a, temperature dependences of the intensities of the Eu^{3+}- (curve 1), Tb^{3+}- (curve 2), and Gd^{3+}- (curve 3) related emissions measured under excitation of the LGSO crystal in the Gd^{3+}-related 4.5 eV absorption band. In the inset of Fig. 6b, temperature dependences of the Ce1- (curve 1) and Eu^{3+}- (curve 2) related emissions in LGSO:Ce.

Fig. 7. Normalized (in the first TSL peak) TSL glow curves measured after X-ray irradiation at 80 K of the (a) nominally undoped LGSO crystal and (b) LGSO:Ce crystal for the Eu^{3+}-related emission (E_{em}=1.85 eV) (solid line) and for the intrinsic, Tb^{3+}-, Ce^{3+}-related emissions (with E_{em}=3.1 eV) (dashed lines).

Fig. 8. Normalized (for the TSL intensity maximum) TSL glow curves measured after X-ray irradiation at 4 K of the (a) nominally undoped LGSO crystal and (b) LGSO:Ce crystal for the Eu^{3+}-related emission (with filter KS-14, solid line), for the intrinsic, Tb^{3+}-, Ce^{3+}-related emissions (with filters ZhS-4+FS-7, dashed lines), and for the ≈3.7 eV emission (with filter UFS-6, dotted line).

Fig. 9. TSL spectra (curves 1-4) measured for the (a) nominally undoped LGSO crystal and (b) LGSO:Ce crystal at different temperatures shown in the legends. In Fig. 9a, the spectra are normalized in the maximum of the Eu^{3+}-related 2.03 eV emission band, and in the E>2.4 eV energy range, the emission intensity is increased 5 times. In Fig. 9b, the spectra are normalized in the maximum of the Ce^{3+}-related emission band (at ≈2.85 eV).

Fig. 10. Dependences of the trap depth values (E_t) on the temperature T_{stop} obtained from the analysis of the TSL glow curves measured (a) for the intrinsic and Tb^{3+}-related (E_{em}=3.2 eV, empty circles) and Eu^{3+}-related (E_{em}=1.85 eV, filled circles) emissions of the nominally undoped LGSO crystal and (b) for the Ce^{3+}-related (E_{em}=2.95 eV, empty circles) and Eu^{3+}-related (E_{em}=1.85 eV, filled circles) emission of the LGSO:Ce crystal X-ray irradiated at 80 K. The average values of E_t and frequency factors f_0 are shown in Table 2.

Figure1

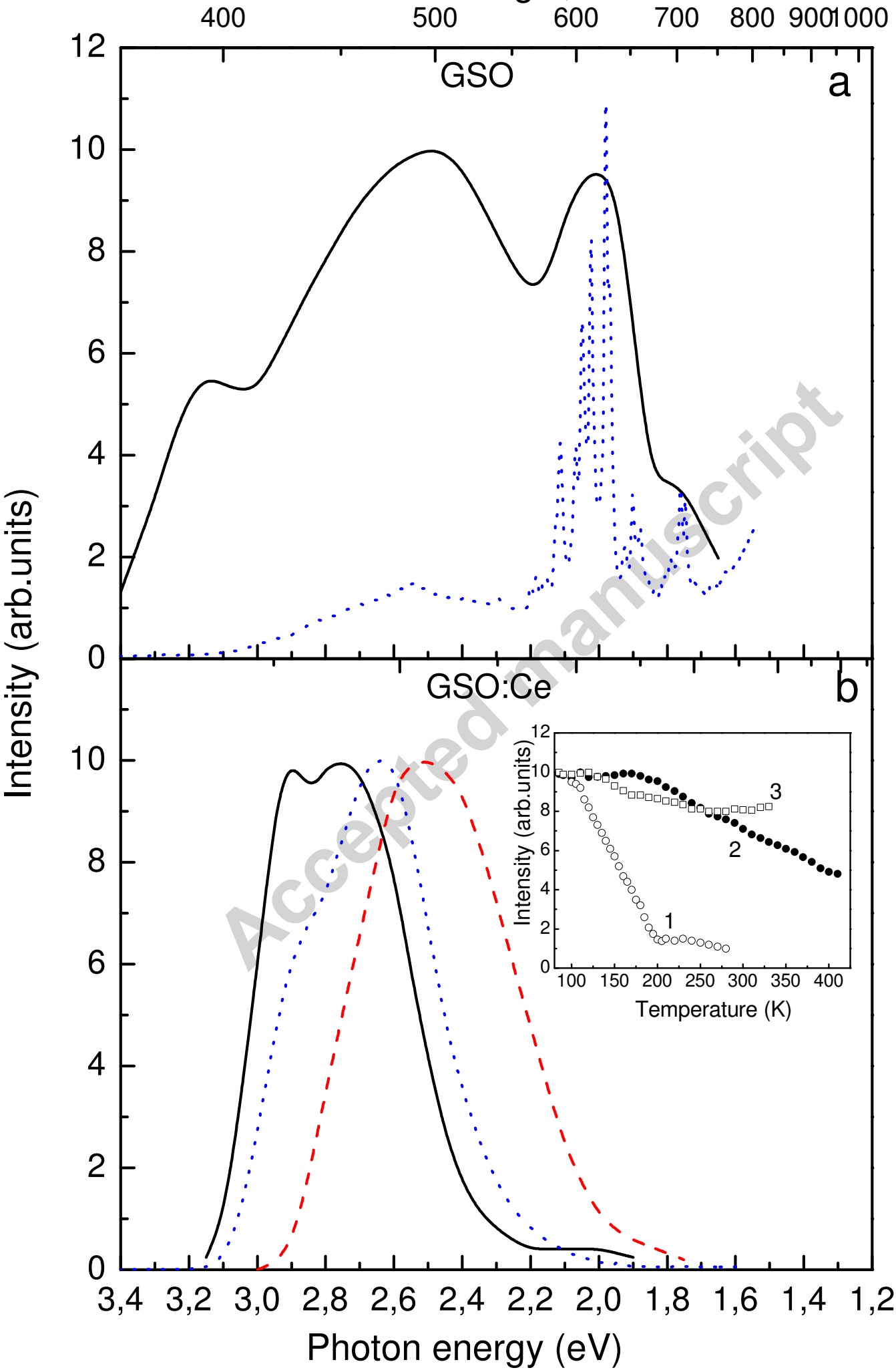

Figure2

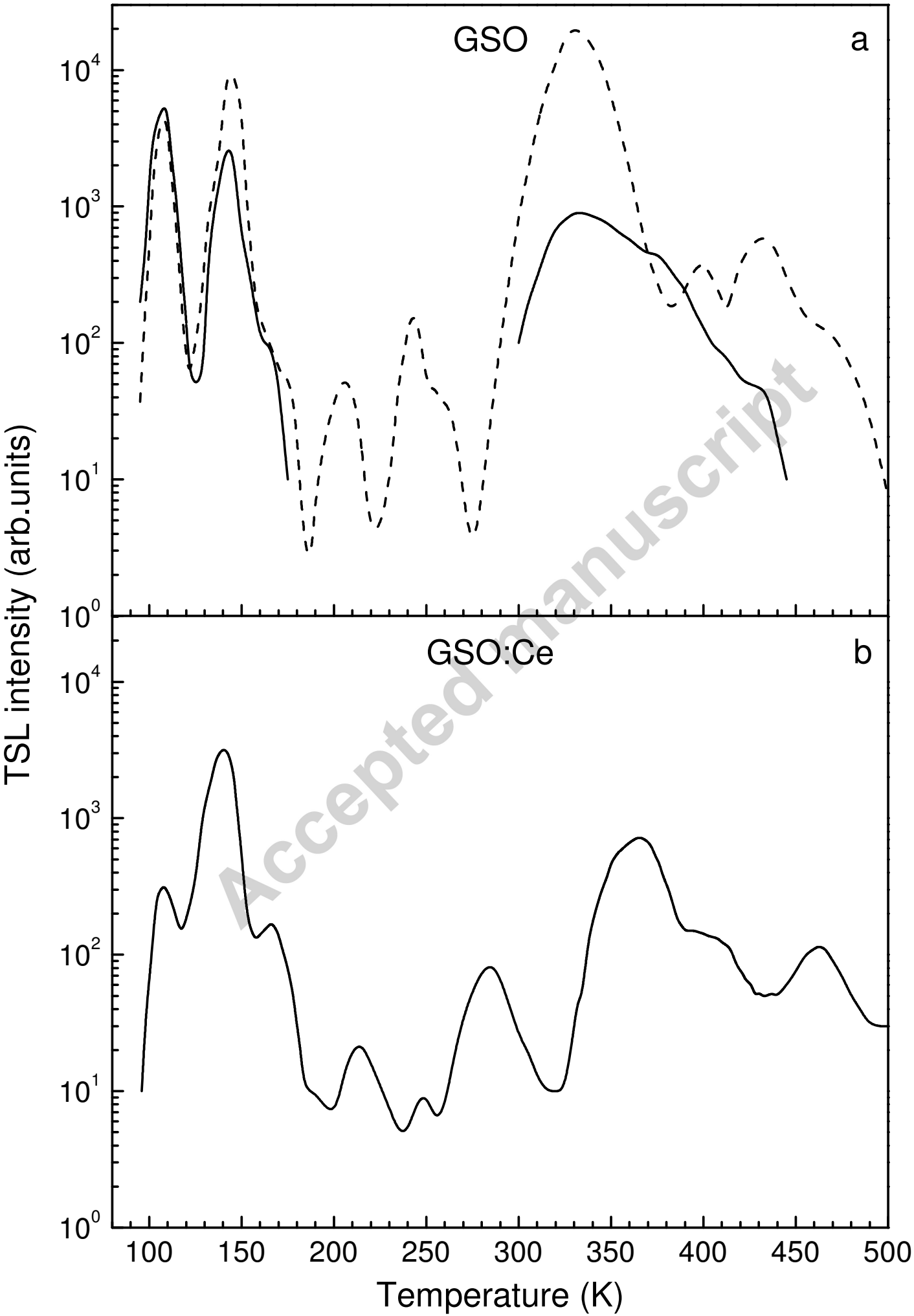

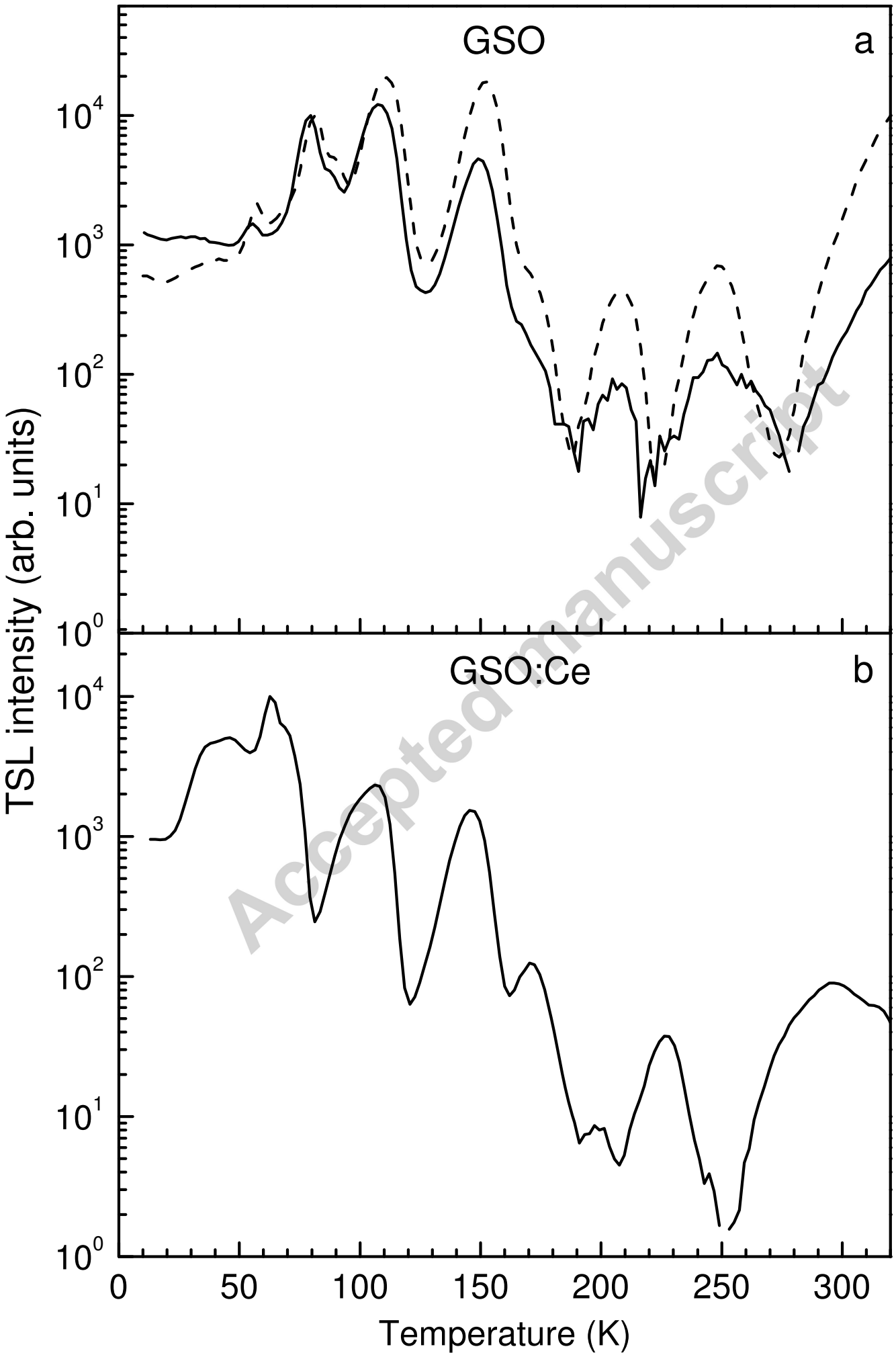

Figure4

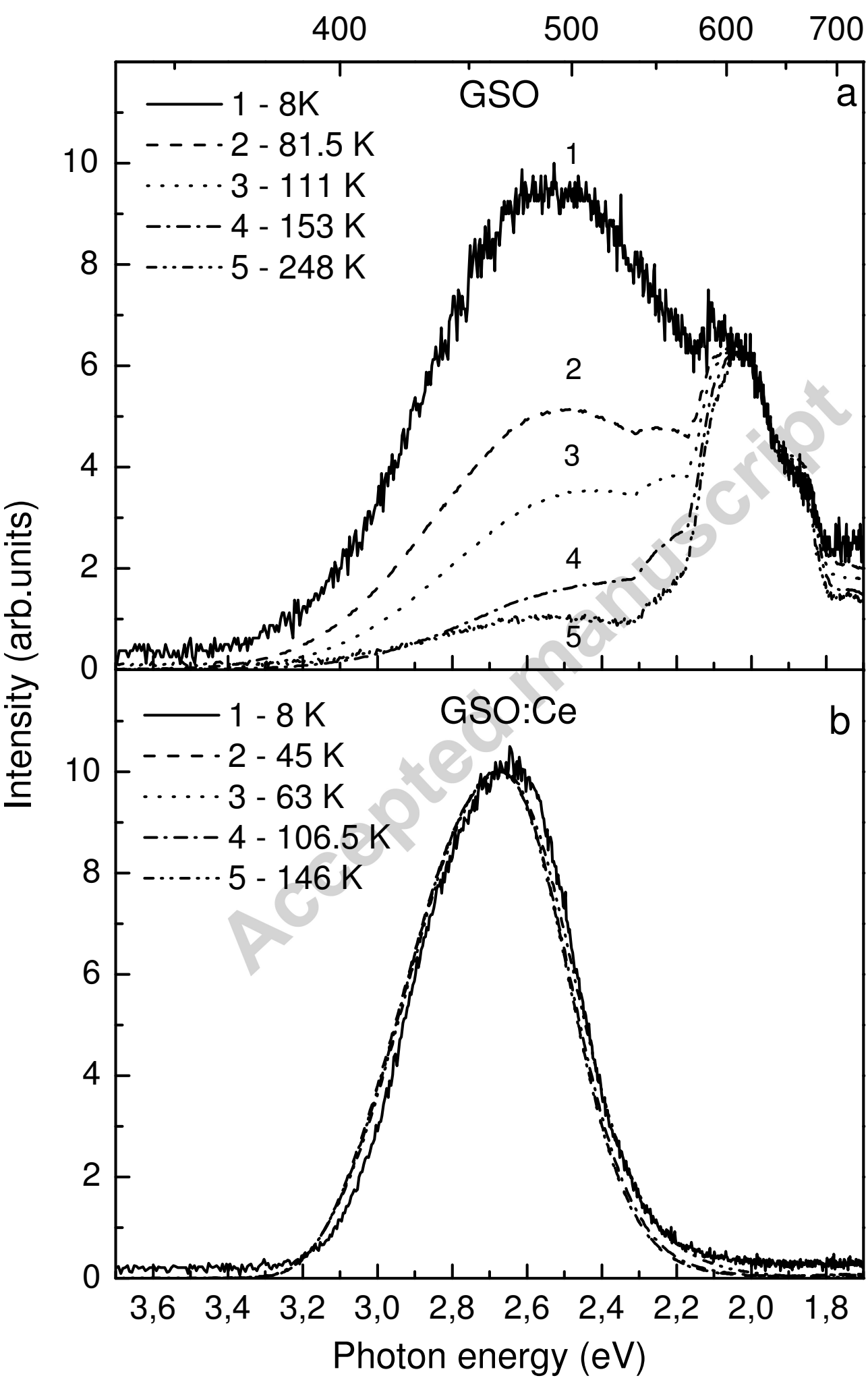

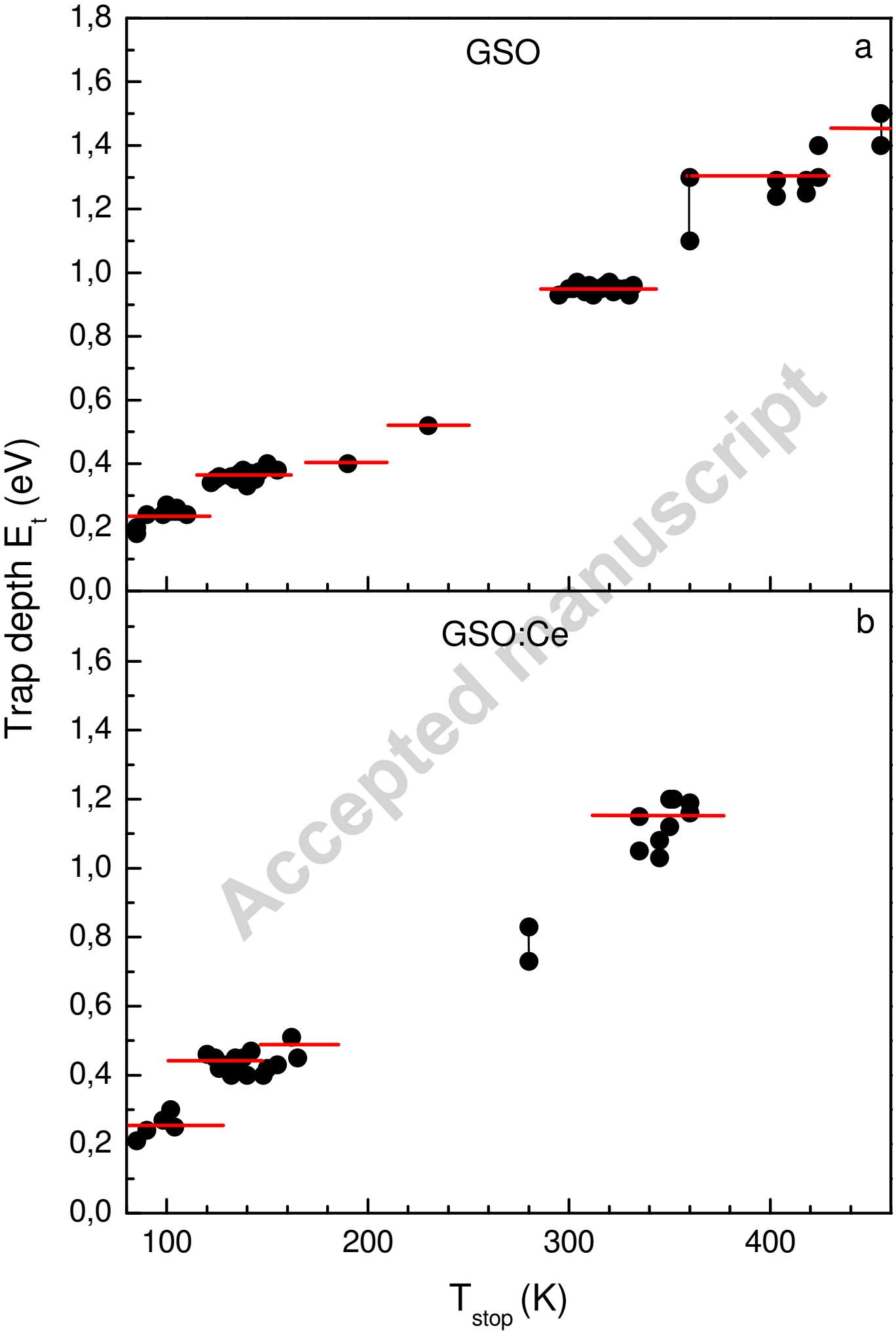

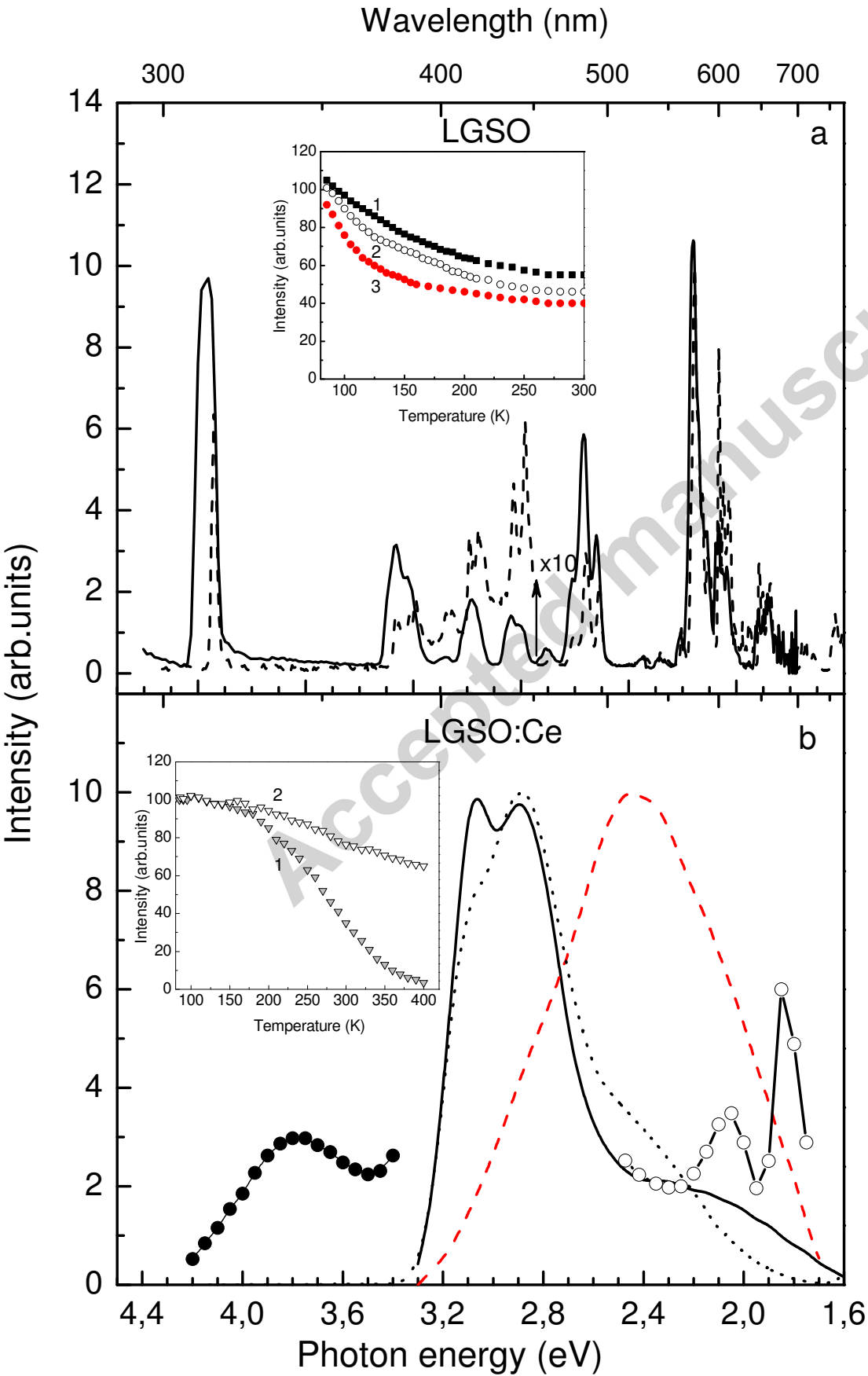

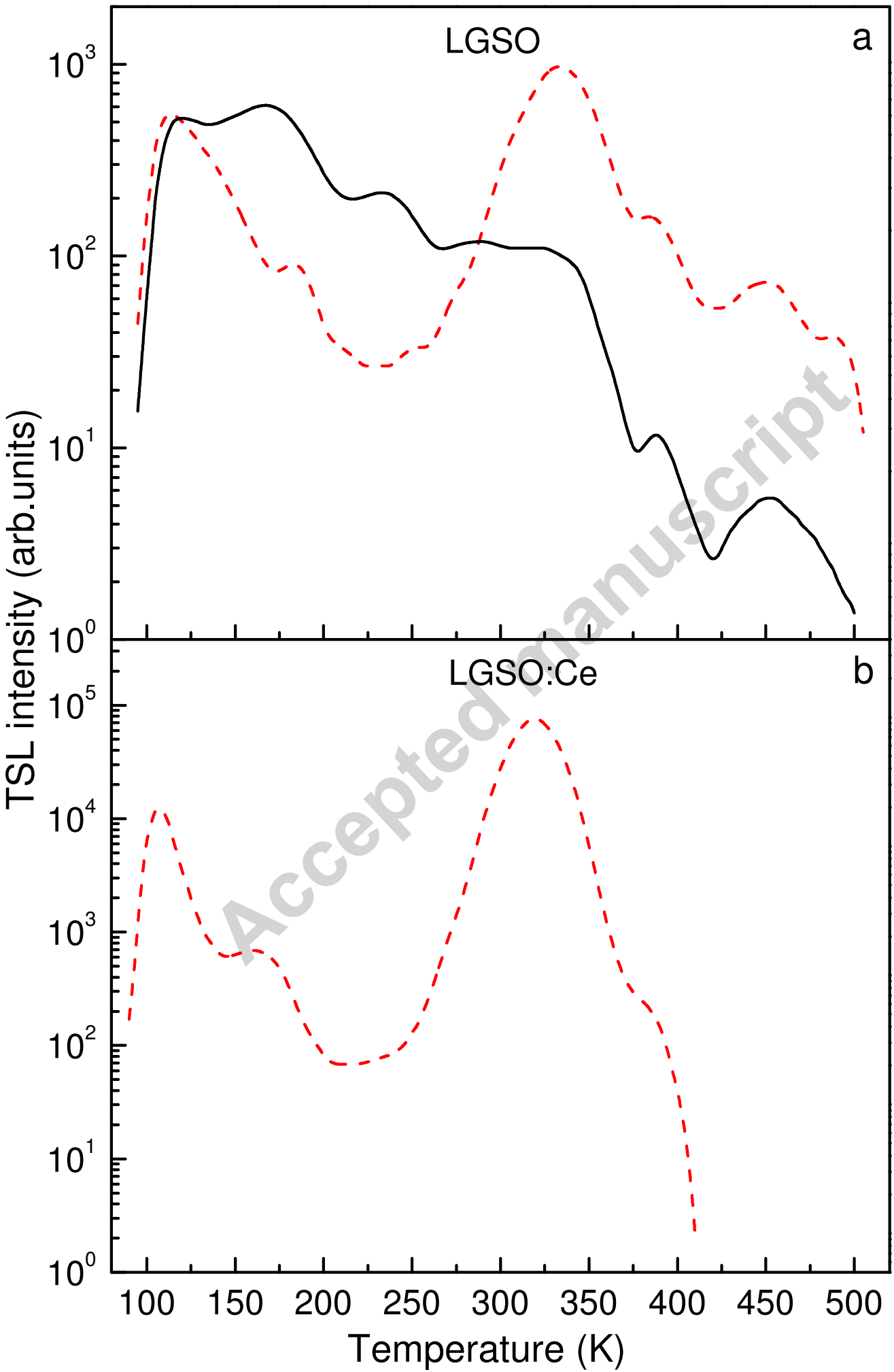

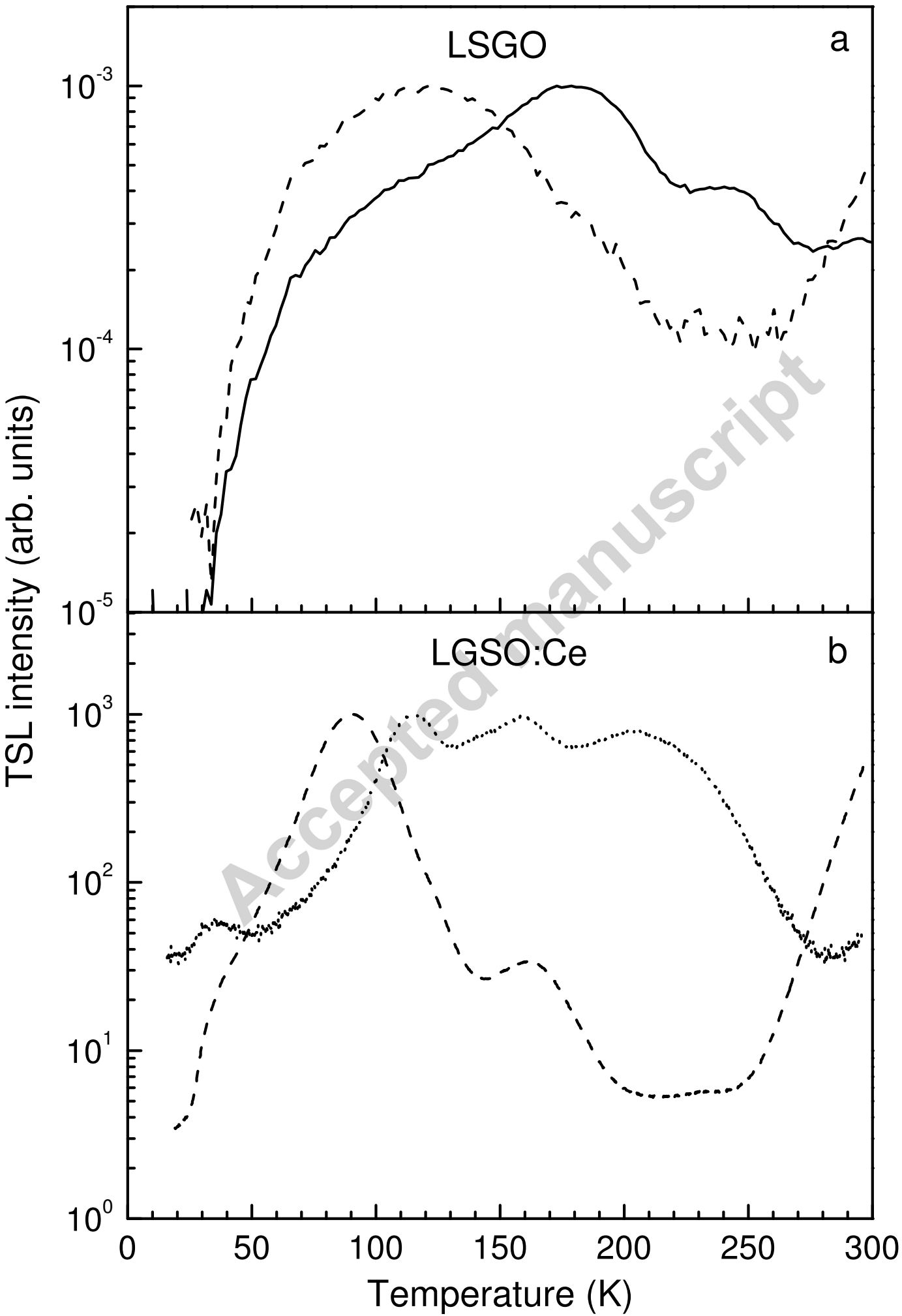

Figure9